True Zero-Speed Low-Jitter High Accuracy Gear Tooth Sensor

Features and Benefits

- Highly repeatable over operating temperature range
- Tight timing accuracy over operating temperature range
- True zero-speed operation
- Air-gap–independent switchpoints
- Vibration immunity
- Large operating air gaps
- Defined power-on state
- Wide operating voltage range
- Digital output representing target profile
- Single-chip sensing IC for high reliability

Continued on the next page…

Package: 4 pin SIP (suffix SG)

Not to scale

Description

The ATS625 true zero-speed gear tooth sensor is an optimized Hall IC and magnet configuration packaged in a molded module that provides a manufacturer-friendly solution for digital gear tooth sensing applications. The sensor assembly consists of an over-molded package that holds together a samarium cobalt magnet, a pole piece concentrator, and a true zero-speed Hall IC that has been optimized to the magnetic circuit. This small package can be easily assembled and used in conjunction with gears of various shapes and sizes.

The sensor incorporates a dual-element Hall IC that switches in response to differential magnetic signals created by a ferrous target. Digital processing of the analog signal provides zero-speed performance independent of air gap as well as dynamic adaptation of device performance to the typical operating conditions found in automotive applications (reduced vibration sensitivity). High-resolution peak detecting DACs are used to set the adaptive switching thresholds of the device. Switchpoint hysteresis reduces the negative effects of any anomalies in the magnetic signal associated with the targets used in many automotive applications. This sensor system is optimized

Continued on the next page…

Functional Block Diagram

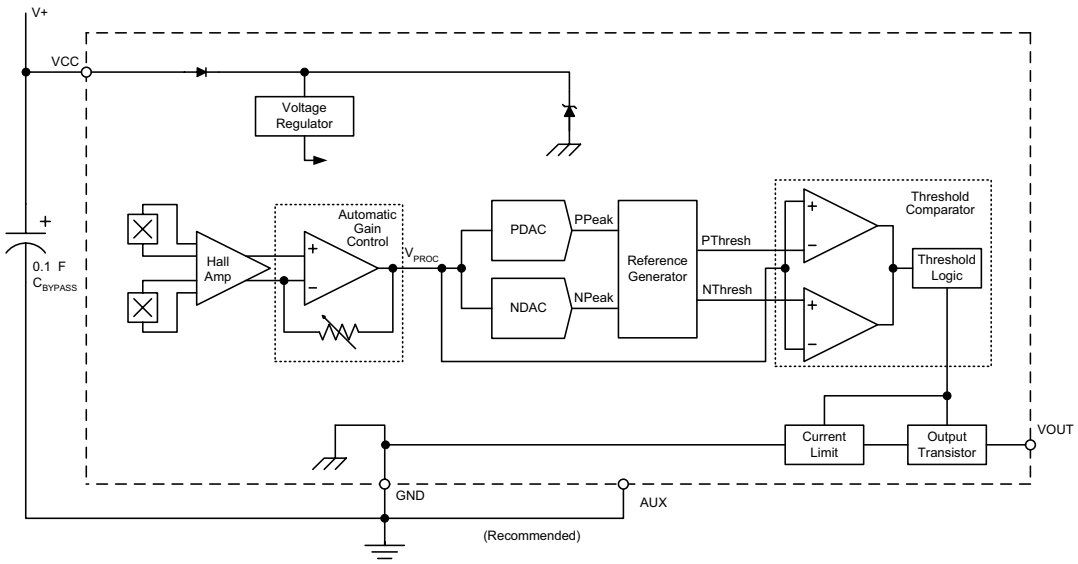

Features and Benefits (continued)

- Small mechanical size
- Optimized Hall IC magnetic system
- Fast start-up
- AGC and reference adjust circuit
- Undervoltage lockout

Description (continued)

for crank applications that utilize targets that possess signature regions.

TheATS625 is provided in a 4-pin SIP. The Pb (lead) free option, available by special request, has a 100% matte tin plated leadframe.

Selection Guide

Part Number	Pb-free[1]	Packing[2]
ATS625LSGTN-T[3]	Yes	Tape and Reel 13-in. 800 pcs./reel

[1]Pb-based variants are being phased out of the product line. Certain variants cited in this footnote are in production but have been determined to be NOT FOR NEW DESIGN. This classification indicates that sale of this device is currently restricted to existing customer applications. The device should not be purchased for new design applications because obsolescence in the near future is probable. Samples are no longer available. Status change: May 1, 2006. These variants include: ATS625LSGTN
[2]Contact Allegro for additional packing options.
[3]Some restrictions may apply to certain types of sales. Contact Allegro for details.

Absolute Maximum Ratings

Characteristic	Symbol	Notes	Rating	Units
Supply Voltage	V_{CC}	See Power Derating section	26.5	V
Reverse-Supply Voltage	V_{RCC}		–18	V
Reverse-Supply Current	I_{RCC}		50	mA
Reverse-Output Voltage	V_{ROUT}		–0.5	V
Output Sink Current	I_{OUT}		10	mA
Operating Ambient Temperature	T_A	Range L	–40 to 150	ºC
Maximum Junction Temperature	T_J(max)		165	ºC
Storage Temperature	T_{stg}		–65 to 170	ºC

Pin-out Diagram

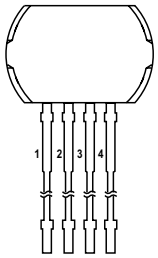

Terminal List

Name	Description	Number
VCC	Connects power supply to chip	1
VOUT	Output from circuit	2
AUX	For Allegro use only	3
GND	Ground	4

Operating Characteristics Valid at T_A = –40°C to 150°C, $T_J \leq T_{J(max)}$, over full range of AG, unless otherwise noted; typical operating parameters: V_{CC} = 12 V and T_A = 25°C

Characteristic	Symbol	Test Conditions	Min.	Typ.	Max.	Units
ELECTRICAL CHARACTERISTICS						
Supply Voltage	V_{CC}	Operating; $T_J < T_{Jmax}$	4.0	–	24	V
Undervoltage Lockout	V_{CCUV}		–	–	< $V_{CC(min)}$	V
Reverse Supply Current	I_{RCC}	V_{CC} = –18 V	–	–	–10	mA
Supply Zener Clamp Voltage[1]	V_Z	I_{CC} = 17 mA	28	–	–	V
Supply Zener Current[2]	I_Z	V_S = 28 V	–	–	17	mA
Supply Current	I_{CC}	Output OFF	–	8.5	14	mA
		Output ON	–	8.5	14	mA
POWER-ON CHARACTERISTICS						
Power-On State	S_{PO}		–	High	–	V
Power-On Time	t_{PO}	Gear Speed < 100 RPM; $V_{CC} > V_{CC}$ min	–	–	200	µs
OUTPUT STAGE						
Low Output Voltage	$V_{OUT(SAT)}$	I_{SINK} = 20 mA, Output = ON	–	200	450	mV
Output Current Limit	$I_{OUT(LIM)}$	V_{OUT} = 12 V, $T_J < T_{Jmax}$	25	45	70	mA
Output Leakage Current	$I_{OUT(OFF)}$	Output = OFF, V_{OUT} = 24 V	–	–	10	µA
Output Rise Time	t_r	R_L = 500 Ω, C_L = 10 pF	–	1.0	2	µs
Output Fall Time	t_f	R_L = 500 Ω, C_L = 10 pF	–	0.6	2	µs
SWITCHPOINT CHARACTERISTICS						
Speed	S	Reference target 60+2	0	–	12000	rpm
Bandwidth	BW	Corresponds to switching frequency – 3 dB	–	20	–	kHz
Operate Point	B_{OP}	% of peak-to-peak signal, AG < AG_{max}; B_{IN} transitioning from LOW to HIGH	–	60	–	%
Release Point	B_{RP}	% of peak-to-peak signal, AG < AG_{max}; B_{IN} transitioning from HIGH to LOW	–	40	–	%
CALIBRATION						
Initial Calibration[3]	Cal_{PO}	Start-up	–	1	6	edges
Calibration Update	Cal	Running mode operation	continuous			–

Continued on the next page...

Operating Characteristics, continued Valid at T_A = –40°C to 150°C, $T_J \le T_{J(max)}$, over full range of AG, unless otherwise noted; typical operating parameters: V_{CC} = 12 V and T_A = 25°C

Characteristic	Symbol	Test Conditions	Min.	Typ.	Max.	Units
OPERATING CHARACTERISTICS with 60+2 reference target						
Operational Air Gap	AG	Measured from sensor branded face to target tooth	0.5	–	2.5	mm
Relative Timing Accuracy, Sequential Mechanical Rising Edges	ERR_{RR}	Relative to measurement taken at AG = 1.5 mm	–	–	±0.4	deg.
Relative Timing Accuracy, Sequential Mechanical Falling Edges	ERR_{FF}	Relative to measurement taken at AG = 1.5 mm	–	–	±0.4	deg.
Relative Timing Accuracy, Signature Mechanical Rising Edge[4]	ERR_{SIGR}	Relative to measurement taken at AG = 1.5 mm	–	–	±0.4	deg.
Relative Timing Accuracy, Signature Mechanical Falling Edge[5]	ERR_{SIGF}	Relative to measurement taken at AG = 1.5 mm	–	–	±1.5	deg.
Relative Repeatability, Sequential Rising and Falling Edges[6]	$T_{\theta E}$	360° Repeatability, 1000 edges; peak-peak sinusoidal signal with $B_{PEAK} \ge B_{IN(min)}$ and 6° period	–	–	0.08	deg.
Operating Signal[7]	B_{IN}	$AG_{(min)} < AG < AG_{(max)}$	60	–	–	G

[1] Test condition is $I_{CC(max)}$ + 3 mA.
[2] Upper limit is $I_{CC(max)}$ + 3 mA.
[3] Power-on speed ≤ 200 rpm. Refer to the *Sensor Description* section for information on start-up behavior.
[4] Detection accuracy of the update algorithm for the first rising mechanical edge following a signature region can be adversely affected by the magnetic bias of the signature region. Please consult with Allegro field applications engineering for aid with assessment of specific target geometries.
[5] Detection accuracy of the update algorithm for the falling edge of the signature region is highly dependent upon specific target geometry. Please consult with Allegro field applications engineering for aid with assessment of specific target geometries.
[6] The repeatability specification is based on statistical evaluation of a sample population.
[7] Peak-to-peak magnetic flux strength required at Hall elements for complying with operational characteristics.

Reference Target (Gear) Information

REFERENCE TARGET 60+2

Characteristics	Symbol	Test Conditions	Typ.	Units	Symbol Key
Outside Diameter	D_o	Outside diameter of target	120	mm	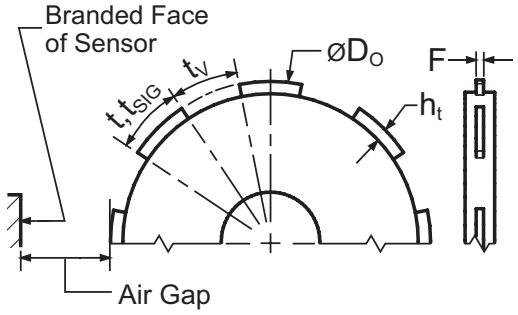
Face Width	F	Breadth of tooth, with respect to sensor	6	mm	
Circular Tooth Length	t	Length of tooth, with respect to sensor; measured at D_o	3	mm	
Signature Region Circular Tooth Length	t_{SIG}	Length of signature tooth, with respect to sensor; measured at D_o	15	mm	
Circular Valley Length	t_v	Length of valley, with respect to sensor; measured at D_o	3	mm	
Tooth Whole Depth	h_t		3	mm	
Material		Low Carbon Steel	–	–	

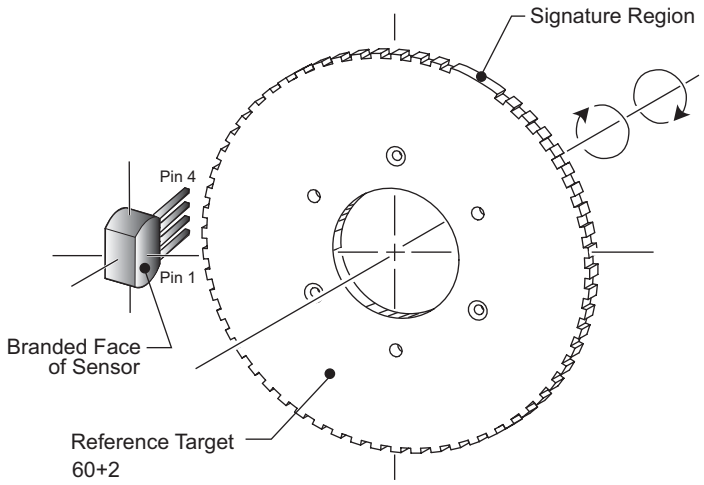

Figure 1. Configuration with Radial-Tooth Reference Target

For the generation of adequate magnetic field levels, the following recommendations should be followed in the design and specification of targets:

- 2 mm < tooth width, t < 4 mm
- Valley width, t_v > 2 mm
- Valley depth, h_t > 2 mm
- Tooth thickness, F ≥ 3 mm
- Target material must be low carbon steel

Although these parameters apply to targets of traditional geometry (radially oriented teeth with radial sensing, shown in figure 1), they also can be applied in applications using stamped targets (an aperture or rim gap punched out of the target material) and axial sensing. For stamped geometries with axial sensing, the valley depth, h_t, is intrinsically infinite, so the criteria for tooth width, t, valley width, t_v, tooth material thickness, F, and material specification need only be considered for reference. For example, F can now be < 3 mm.

Characteristic Data: Electrical

$I_{CC(ON)}$ Versus V_{CC}

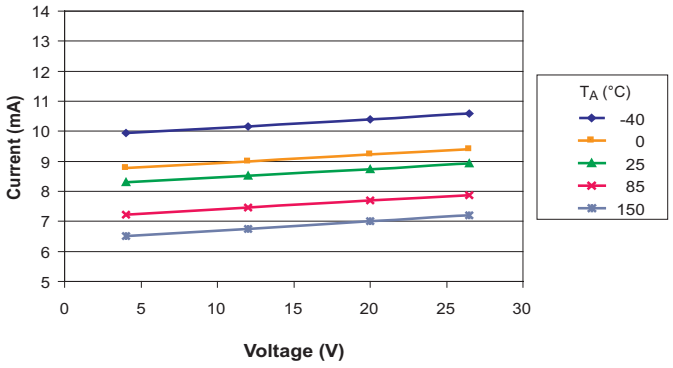

$I_{CC(ON)}$ Versus T_A

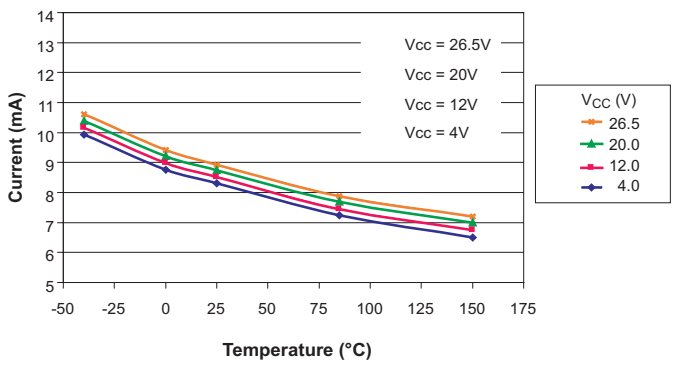

$I_{CC(OFF)}$ Versus V_{CC}

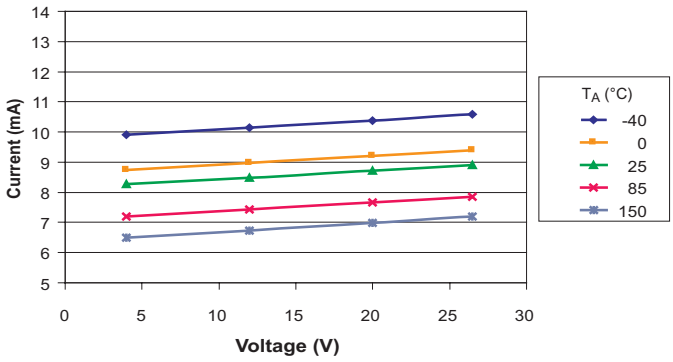

$I_{CC(OFF)}$ Versus T_A

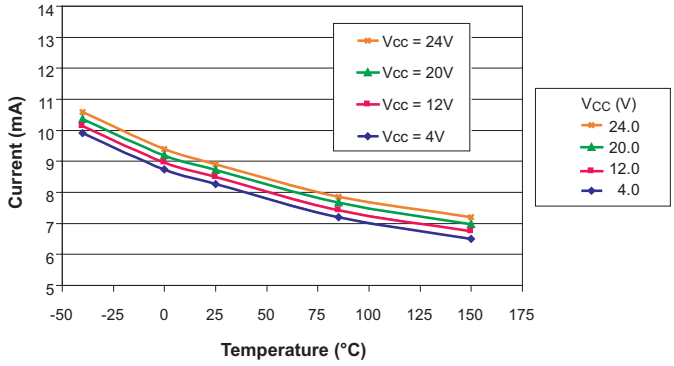

$I_{OUT(OFF)}$ Versus T_A

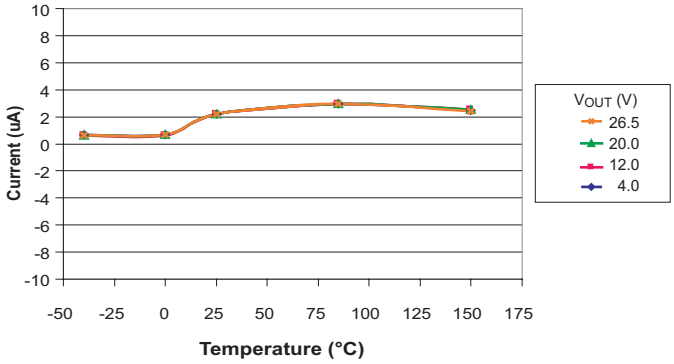

$V_{OUT(SAT)}$ Versus T_A

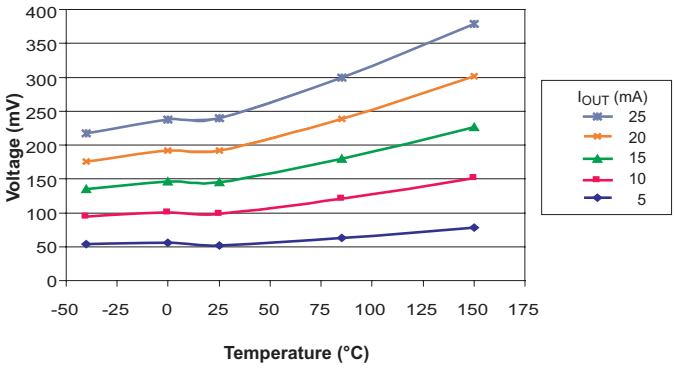

Characteristic Data: Relative Timing Accuracy

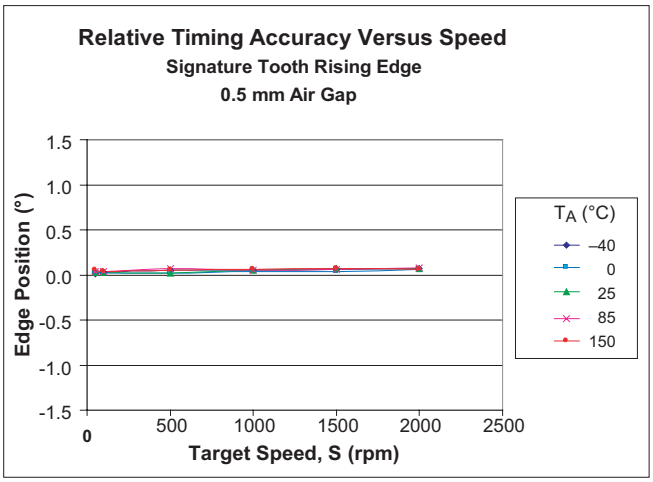

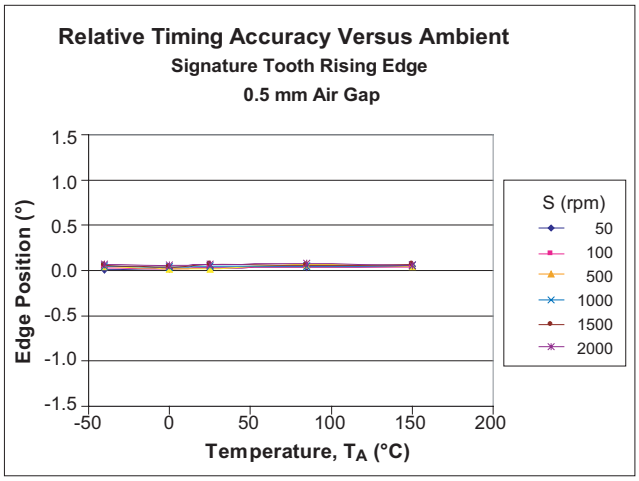

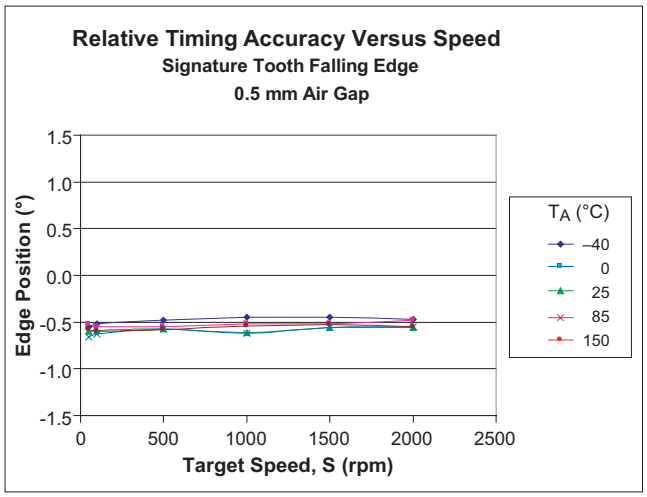

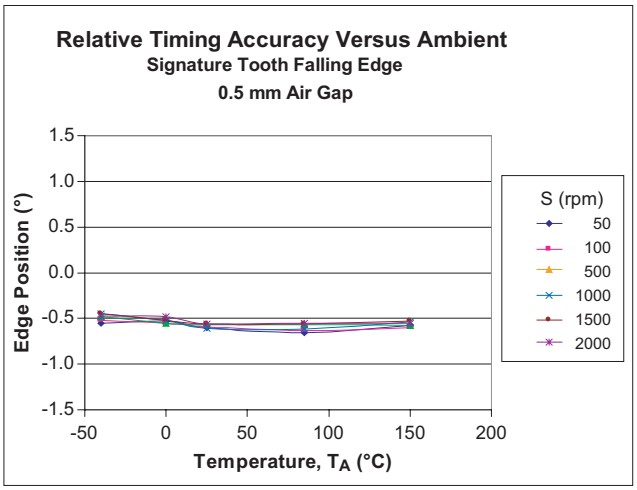

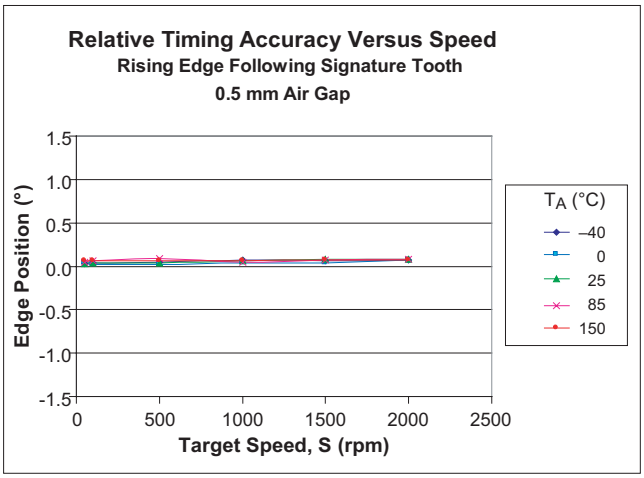

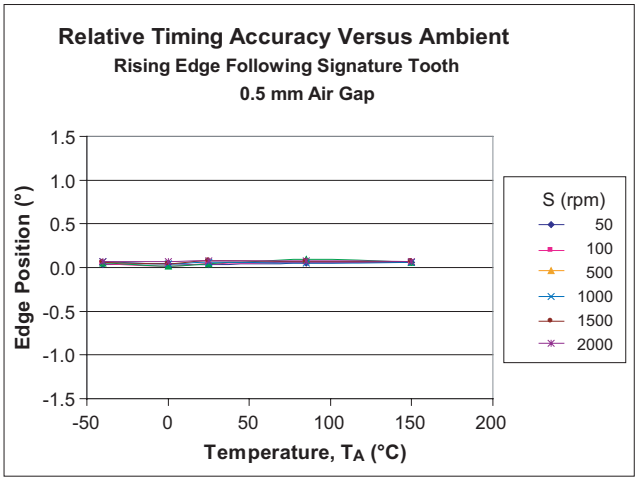

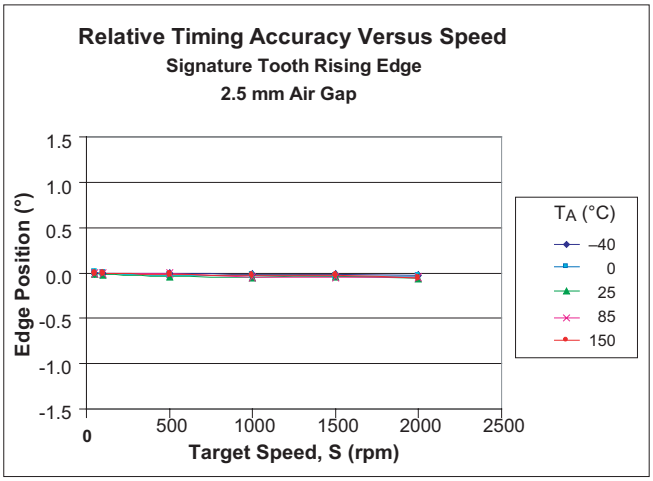
Relative Timing Accuracy Versus Speed
Signature Tooth Rising Edge
2.5 mm Air Gap
Edge Position (°)
1.5
1.0
0.5
0.0
-0.5
-1.0
-1.5
0
500
1000
1500
2000
2500
Target Speed, S (rpm)
TA (°C)
–40
0
25
85
150

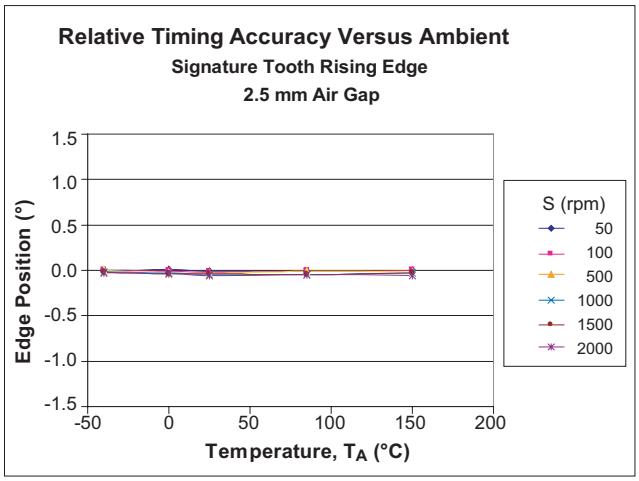
Relative Timing Accuracy Versus Ambient
Signature Tooth Rising Edge
2.5 mm Air Gap
Edge Position (°)
1.5
1.0
0.5
0.0
-0.5
-1.0
-1.5
-50
0
50
100
150
200
Temperature, TA (°C)
S (rpm)
50
100
500
1000
1500
2000

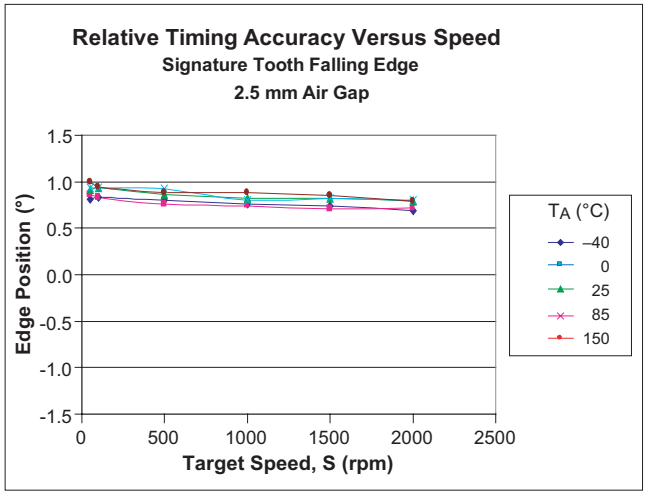
Relative Timing Accuracy Versus Speed
Signature Tooth Falling Edge
2.5 mm Air Gap
Edge Position (°)
1.5
1.0
0.5
0.0
-0.5
-1.0
-1.5
0
500
1000
1500
2000
2500
Target Speed, S (rpm)
TA (°C)
–40
0
25
85
150

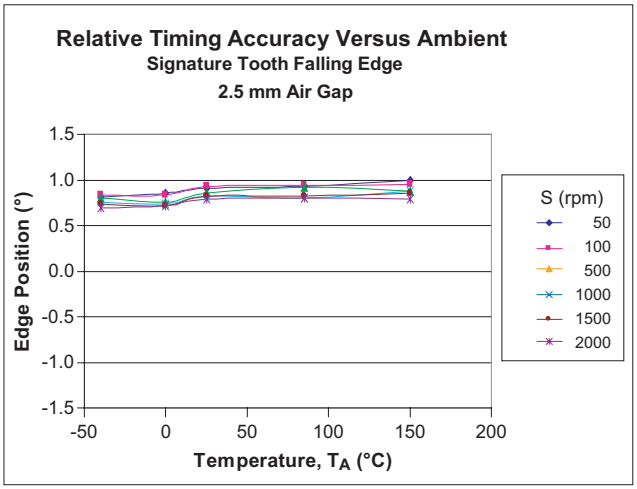
Relative Timing Accuracy Versus Ambient
Signature Tooth Falling Edge
2.5 mm Air Gap
Edge Position (°)
1.5
1.0
0.5
0.0
-0.5
-1.0
-1.5
-50
0
50
100
150
200
Temperature, TA (°C)
S (rpm)
50
100
500
1000
1500
2000

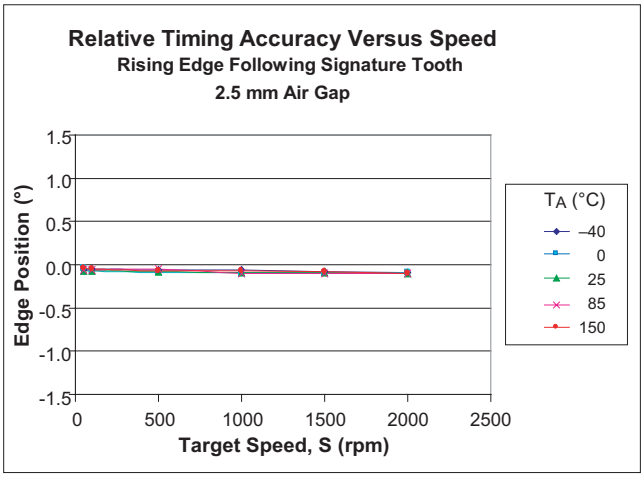
Relative Timing Accuracy Versus Speed
Rising Edge Following Signature Tooth
2.5 mm Air Gap
Edge Position (°)
1.5
1.0
0.5
0.0
-0.5
-1.0
-1.5
0
500
1000
1500
2000
2500
Target Speed, S (rpm)
TA (°C)
–40
0
25
85
150

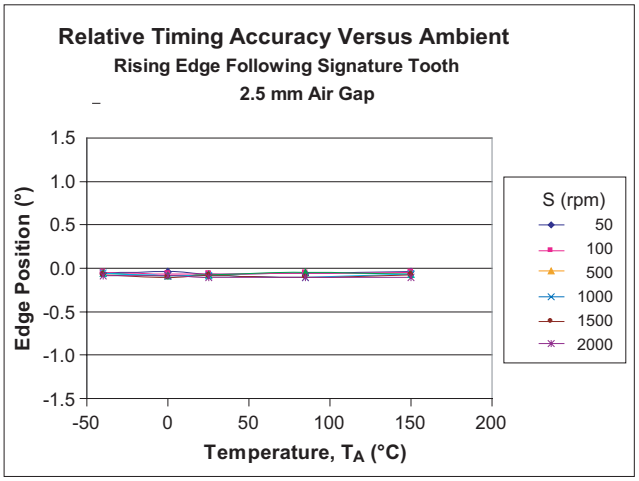
Relative Timing Accuracy Versus Ambient
Rising Edge Following Signature Tooth
2.5 mm Air Gap
Edge Position (°)
1.5
1.0
0.5
0.0
-0.5
-1.0
-1.5
-50
0
50
100
150
200
Temperature, TA (°C)
S (rpm)
50
100
500
1000
1500
2000

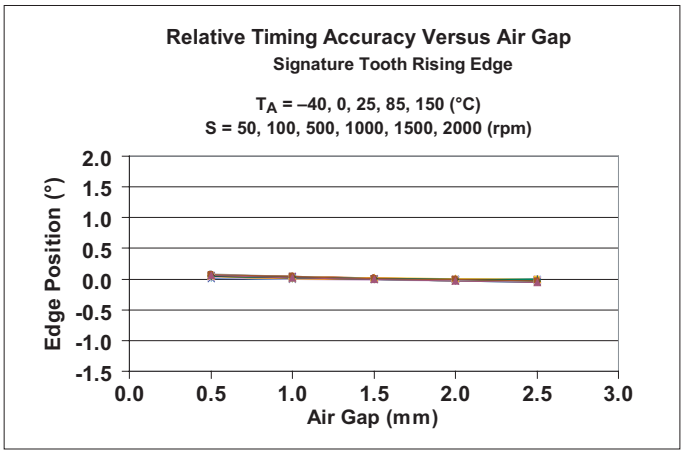

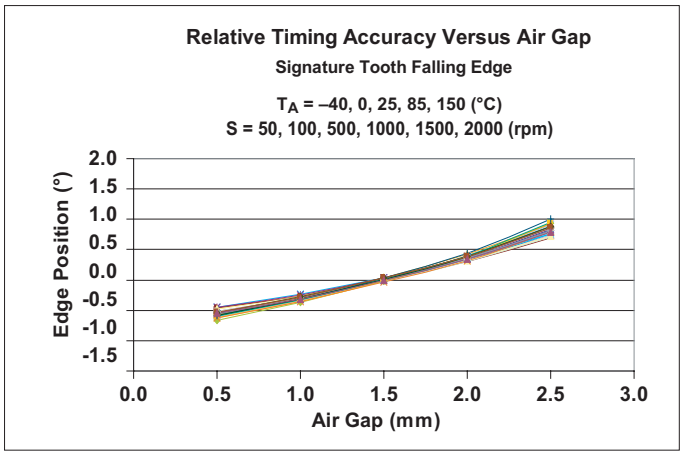

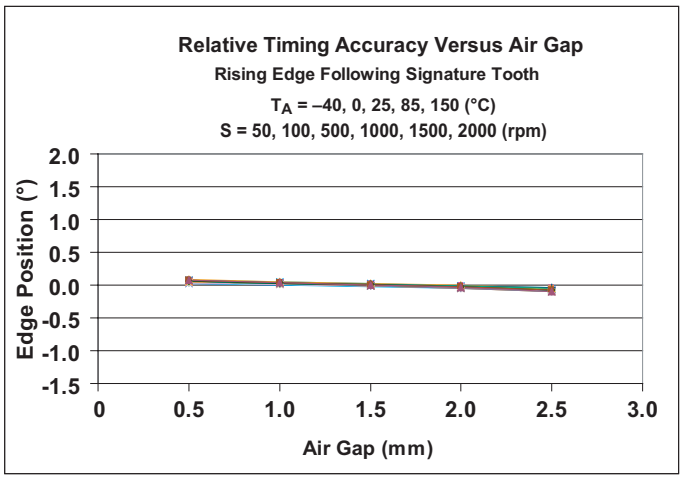

Characteristic Data: Repeatability

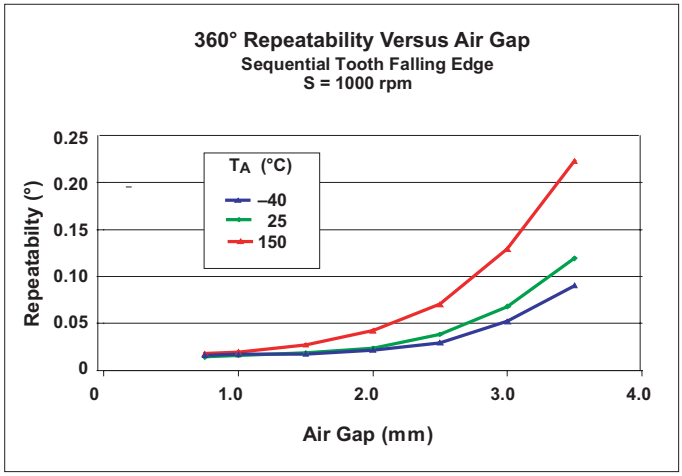

Sensor Description

Assembly Description

The ATS625LSG true zero-speed gear tooth sensor is a combined Hall IC-magnet configuration that is fully optimized to provide digital detection of gear tooth edges. This sensor is integrally molded into a plastic body that has been optimized for size, ease of assembly, and manufacturability. High operating temperature materials are used in all aspects of construction.

Sensing Technology

The gear tooth sensor contains a single-chip differential Hall effect sensor IC, a 4-pin leadframe, a samarium cobalt magnet, and a flat ferrous pole piece. The Hall IC consists of two Hall elements spaced 2.2 mm apart, and each independently measures the magnetic gradient created by the passing of a ferrous object. This is illustrated in figures 2 and 3. The differential output of the two elements is converted to a digital signal that is processed to provide the digital output.

Switching Description

After proper power is applied to the component, the sensor is then capable of providing digital information that is representative of the profile of a rotating gear, as illustrated in figure 4. No additional optimization is needed and minimal processing circuitry is required. This ease of use reduces design time and incremental assembly costs for most applications.

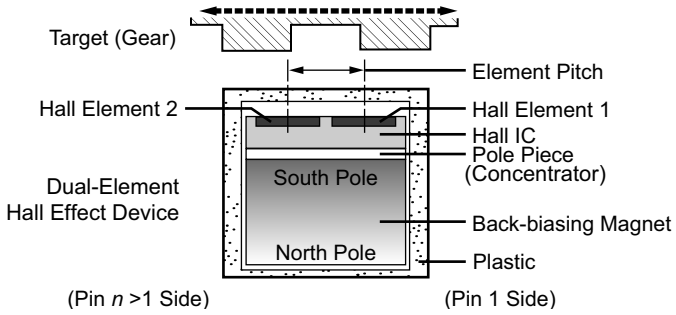

Figure 2. Device Cross Section. Relative motion of the target is detected by the dual Hall elements mounted on the Hall IC. This view is from the side opposite the pins.

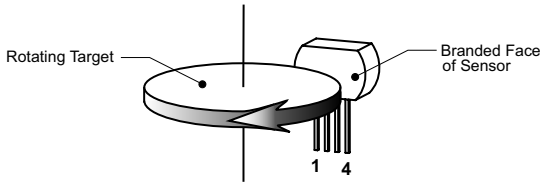

Figure 3. This left-to-right (pin 1 to pin 4) direction of target rotation results in a high output signal when a tooth of the target gear is centered over the face of the sensor. A right-to-left (pin 4 to pin 1) rotation inverts the output signal polarity.

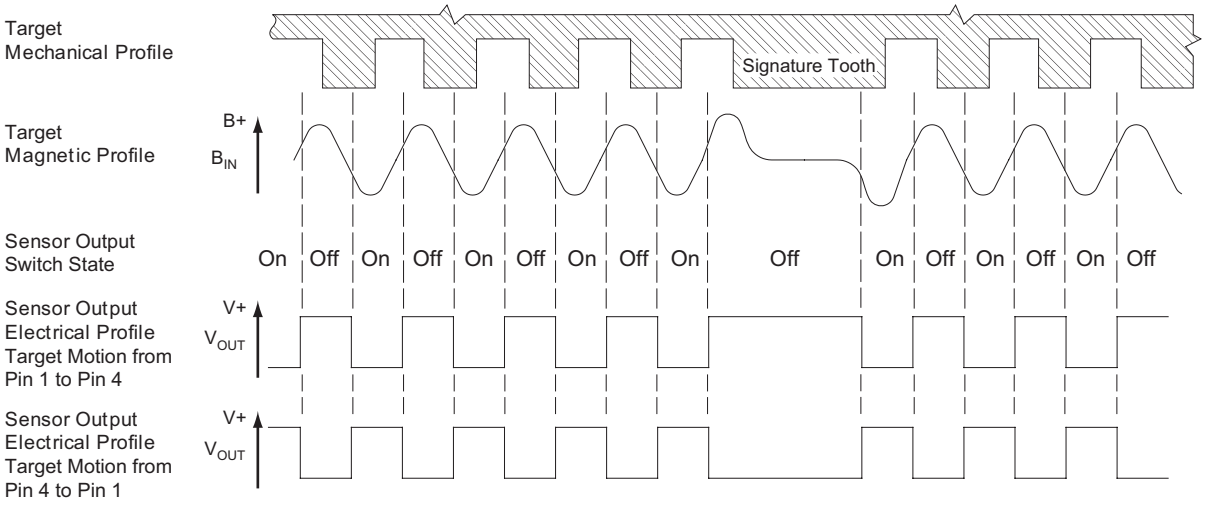

Figure 4. The magnetic profile reflects the geometry of the target, allowing the device to present an accurate digital output response.

Undervoltage Lockout

When the supply voltage falls below the undervoltage lockout level, V_{CCUV}, the device switches to the OFF state. The device remains in that state until the voltage level is restored to to the V_{CC} operating range. Changes in the target magnetic profile have no effect until voltage is restored. This prevents false signals caused by undervoltage conditions from propagating to the output of the sensor.

Power Supply Protection

The device contains an on-chip regulator and can operate over a wide range of supply voltage levels. For applications using an unregulated power supply, transient protection must be added externally. For applications using a regulated supply line, EMI and RFI protection may still be required. The circuit shown in figure 5 is the basic configuration required for proper device operation. Contact Allegro field applications engineering for information on the circuitry required for compliance to various EMC specifications.

Internal Electronics

The ATS625LSG contains a self-calibrating Hall effect IC that possesses two Hall elements, a temperature compensated amplifier and offset cancellation circuitry. The IC also contains a voltage regulator that provides supply noise rejection over the operating voltage range. The Hall transducers and the electronics are integrated on the same silicon substrate by a proprietary BiCMOS process. Changes in temperature do not greatly affect this device due to the stable amplifier design and the offset rejection circuitry.

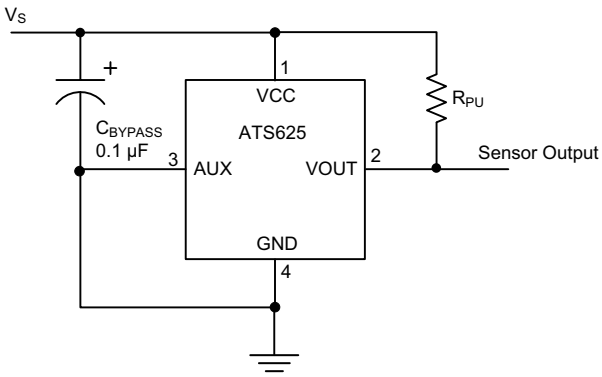

Figure 5. Power Supply Protection Typical Circuit

Sensor Operation Description

Power-On State

At power-on, the device is guaranteed to initialize in the OFF state, with V_{OUT} high.

First Edge Detection

The device uses the first two mechanical edges to synchronize with the target features (tooth or valley) and direction of rotation of the target. The device is synchonized by the third edge. The actual behavior is affected by: target rotation direction relative to the, target feature (tooth, rising edge, falling edge, or valley) that is centered on the device at power-on, and fact that the sensor powers-on in the OFF state,with V_{OUT} high, regardless of the eventual direction of target rotation. The interaction of these factors results in a number of possible power-on scenarios. These are diagrammed in figure 6. In all start-up scenarios, the correct number of output edges is provided, but the accuracy of the first two edges may be compromised.

(A) Target relative movement as shown in figure 3. Output signal is high over the tooth.

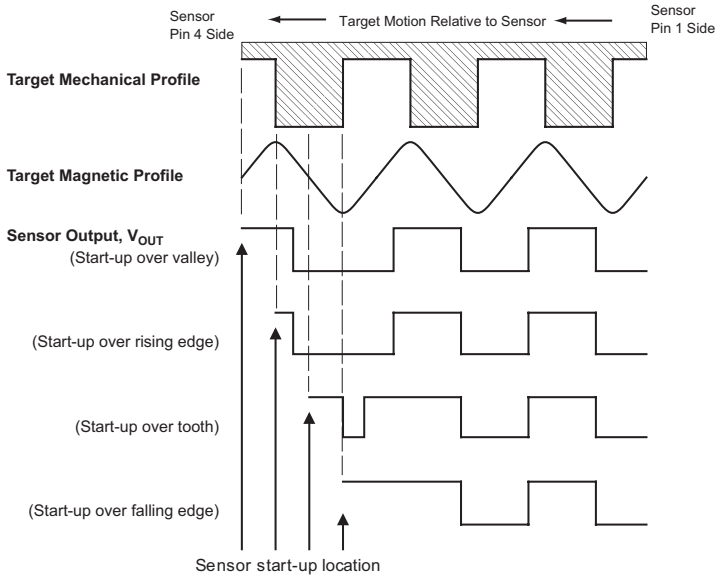

(B) Target relative movement opposite that shown in figure 3. Output signal is low over the tooth.

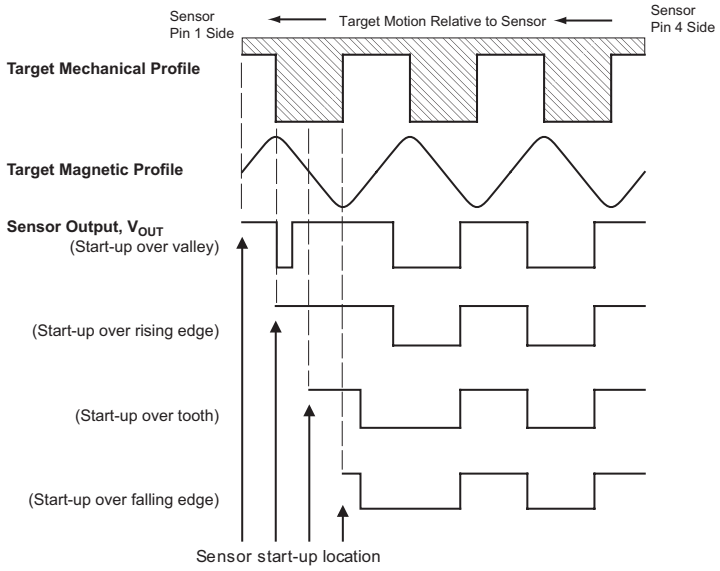

Figure 6. Start-up Position And Relative Motion Effects on First Device Output Switching. Panel A shows the effects when the target is moving from pin 1 toward pin 4 of the device; V_{OUT} goes high at the approach of a tooth. When the target is moving in the opposite direction, as in panel B, the polarity of the device output inverts; V_{OUT} goes low at the approach of a tooth.

AGC (Automatic Gain Control)

The AGC feature is implemented by a unique patented self-calibrating circuitry. After each power-on, the device measures the peak-to-peak magnetic signal. The gain of the sensor is then adjusted, keeping the internal signal amplitude constant over the air gap range of the device, AG. This feature ensures that operational characteristics are isolated from the effects of changes in AG. The effect of AGC is shown in figure 7.

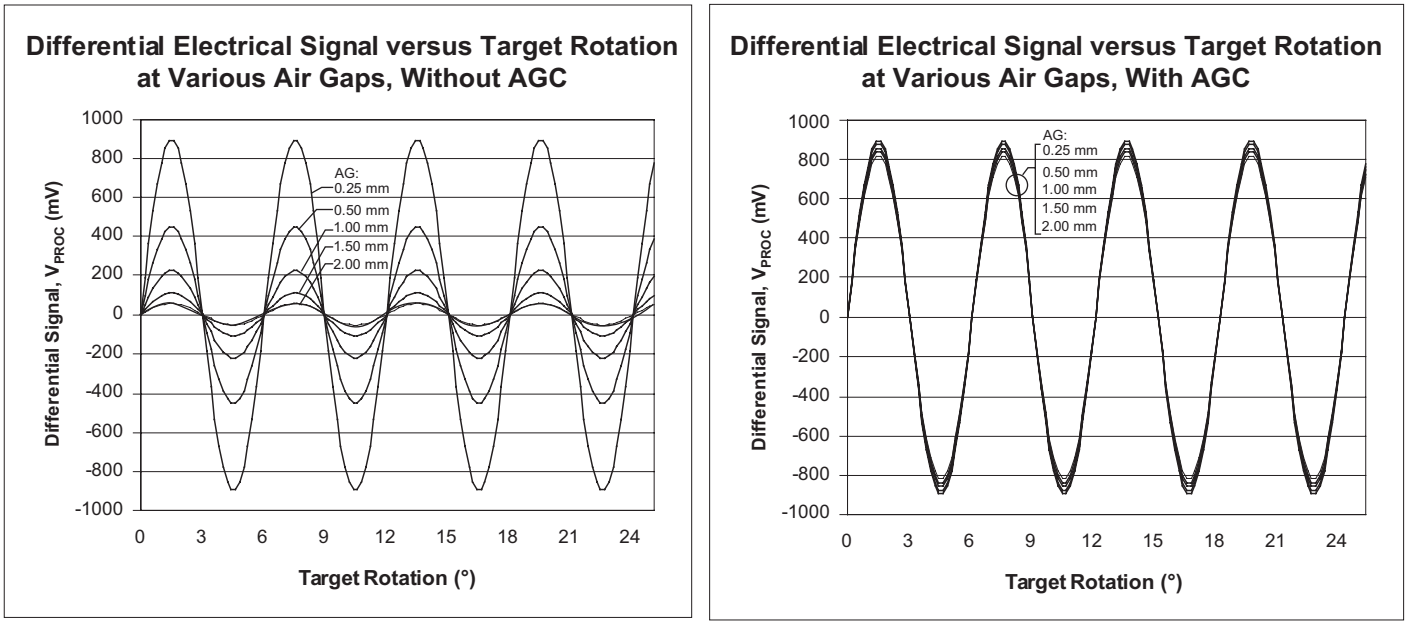

Figure 7. Effect of AGC. The left panel shows the process signal, V_{PROC}, without AGC. The right panel shows the effect with AGC. The result is a normalized V_{PROC}, which allows optimal performance by the rest of the circuits that reference this signal.

Offset Adjustment

In addition to normalizing performance over varying AG, the gain control circuitry also reduces the effect of chip, magnet, and installation offsets. This is accomplished using two DACs (D to A converters) that capture the peaks and valleys of the processed signal, V_{PROC}, and use it as a reference for the Threshold Comparator subcircuit, which controls device switching. If induced offsets bias the absolute signal up or down, AGC and the dynamic DAC behavior work to normalize and reduce the impact of the offset on sensor performance.

SWITCHPOINTS

Switchpoints in the ATS625 are a percentage of the amplitude of the signal, V_{PROC}, after normalization with AGC. In operation, the actual switching levels are determined dynamically. Two DACs track the peaks of V_{PROC} (see the *Update* subsection). The switching thresholds are established at 40% and 60% of the values held in the two DACs. The proximity of the thresholds near the 50% level ensures the most accurate and consistent switching, because it is where the slope of V_{PROC} is steepest and least affected by air gap variation.

The low hysteresis, 20%, provides high performance over various air gaps and immunity to false switching on noise, vibration, backlash, or other transient events.

Figure 8 graphically demonstrates the establishment of the switching threshold levels.Because the thresholds are established dynamically as a percentage of the peak-to-peak signal, the effect of a baseline shift is minimized. As a result, the effects of offsets induced by tilted or off-center installation are minimized.

UPDATE

The ATS625 incorporates an algorithm that continuously monitors the system and updates the switching thresholds accordingly. The switchpoint for each edge is determined by the signal resulting from the previous two edges. Because variations are tracked in real time, the sensor has high immunity to target run-out and retains excellent accuracy and functionality in the presence of both run-out and transient mechanical events. Figure 9 shows how the sensor uses historical data to provide the switching threshold for a given edge.

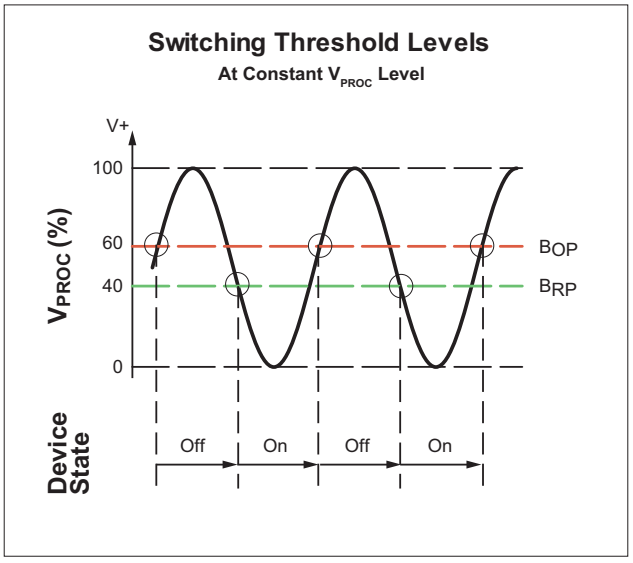

Figure 8. Switchpoint Relationship to Thresholds.The device switches when V_{PROC} passes a threshold level, B_{OP} or B_{RP}, while changing in the corresponding direction: increasing for a B_{OP} switchpoint, and decreasing for a B_{RP} switchpoint.

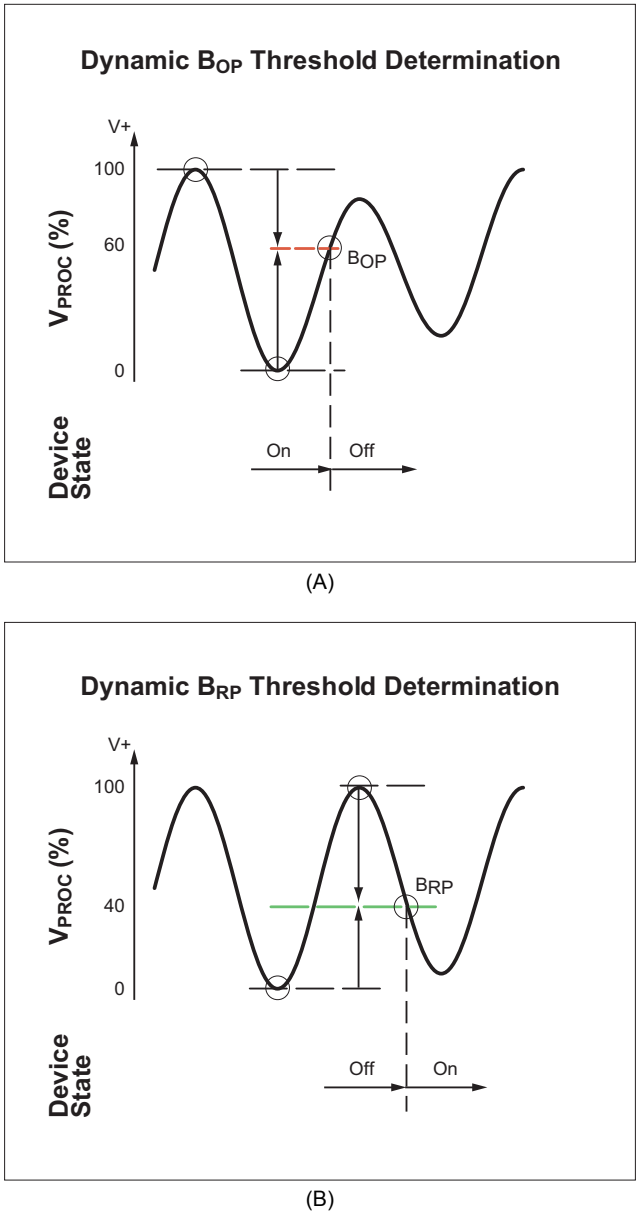

Figure 9. Switchpoint Determination. The two previous V_{PROC} peaks are used to determine the next threshold level: panel A, operate point, and panel B, release point.

Sensor and Target Evaluation

Magnetic Profile

In order to establish the proper operating specification for a particular sensor and target system, a systematic evaluation of the magnetic circuit should be performed. The first step is the generation of a magnetic map of the target. By using a calibrated device, a magnetic profile of the system is made. Figure 10 is a magnetic map of the 60+2 reference target.

A single curve can be derived from this map data, and be used to describe the peak-to-peak magnetic field strength versus the size of the air gap, AG. This allows determination of the minimum amount of magnetic flux density that guarantees operation of the sensor, B_{IN}, so the system designer can determine the maximum allowable AG for the sensor and target system. Referring to figure 11, a B_{IN} of 60 G corresponds to a maximum AG of approximately 2.5 mm.

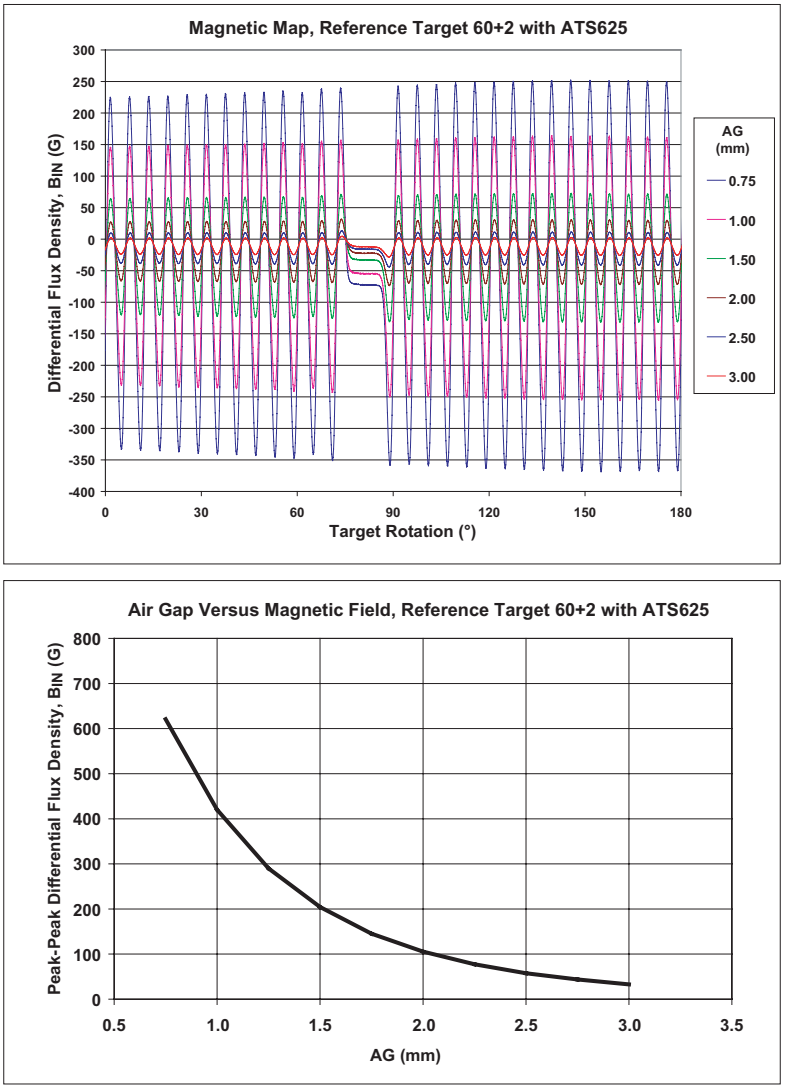

Figure 10. Magnetic Data for the Reference Target 60+2 with ATS625. In the top panel, the Signature Region appears in the center of the plot.

ACCURACY

While the update algorithm will allow the sensor to adapt to typical air gap variations, major changes in air gap can adversely affect switching performance. When characterizing sensor performance over a significant air gap range, be sure to re-power the device at each test at different air gaps. This ensures that self-calibration occurs for each installation condition. See the *Operating Characteristics* table and the charts in the *Characteristic Data: Relative Timing Accuracy* section for performance information.

REPEATABILITY

Repeatability measurement methodology has been formulated to minimize the effect of test system jitter on device measurements. By triggering the measurement instrument, such as an oscilloscope, close to the desired output edge, the speed variations that occur within a single revolution of the target are effectively nullified. Because the trigger event occurs a very short time before the measured event, little opportunity is given for measurement system jitter to impact the time-based measurements.

After the data is taken on the oscilloscope, statistical analysis of the distribution is made to quantify variability and capability. Although complete repeatability results can be found in the *Characteristic Data: Repeatability* section, figure 11 shows the correlation between magnetic signal strength and repeatability. Because an direct relationship exists between magnetic signal strength and repeatability, optimum repeatability performance can be attained through minimizing the operating air gap and optimizing the target design.

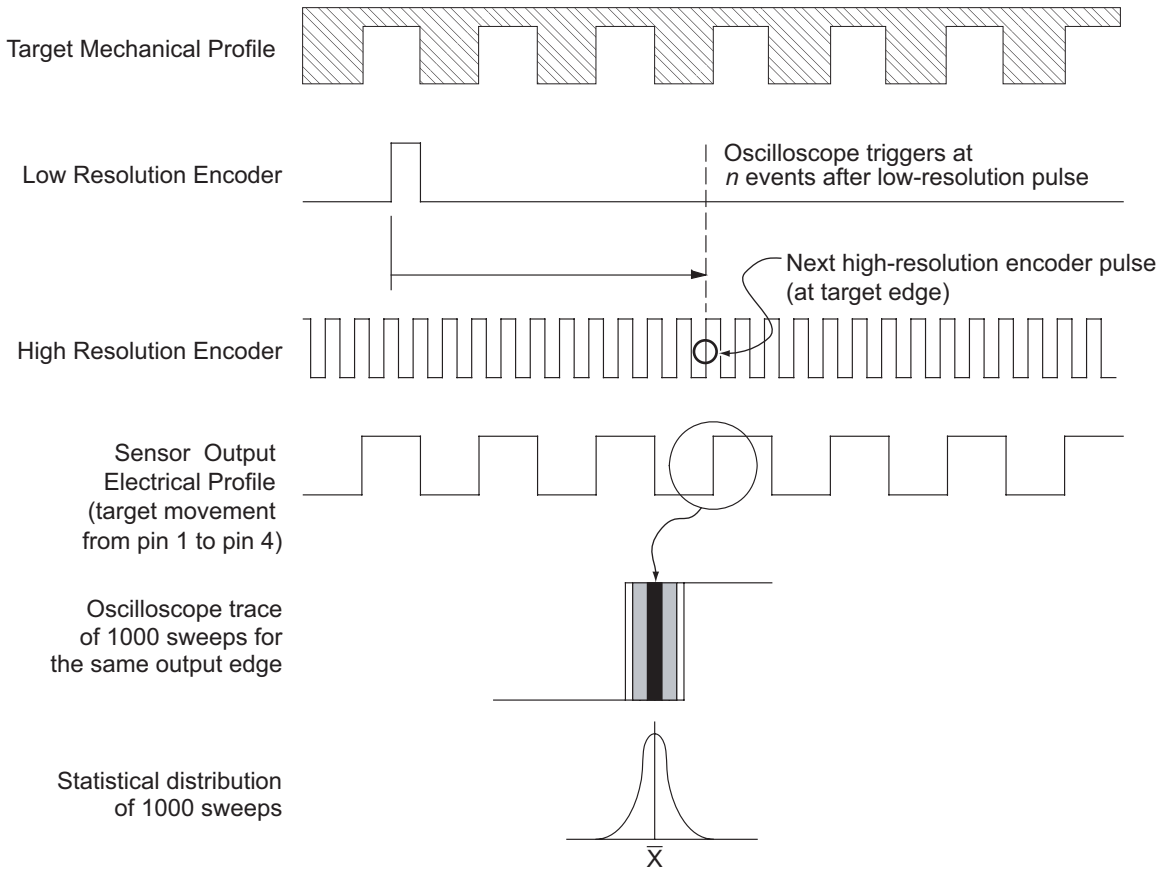

Figure 11. Repeatability Measurement Methodology

Power Derating

THERMAL CHARACTERISTICS may require derating at maximum conditions, see application information

Characteristic	Symbol	Test Conditions*	Value	Units
Package Thermal Resistance	$R_{\theta JA}$	Minimum-K PCB (single layer, single-sided, with copper limited to solder pads)	126	°C/W
		Low-K PCB (single-layer, single-sided with copper limited to solder pads and 3.57 in.^{2} (23.03 cm^2) of copper area each side)	84	°C/W

*Additional information is available on the Allegro Web site.

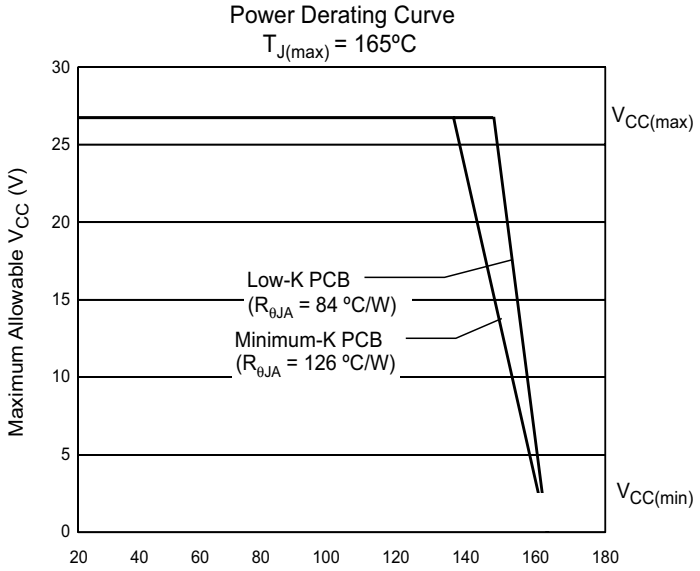

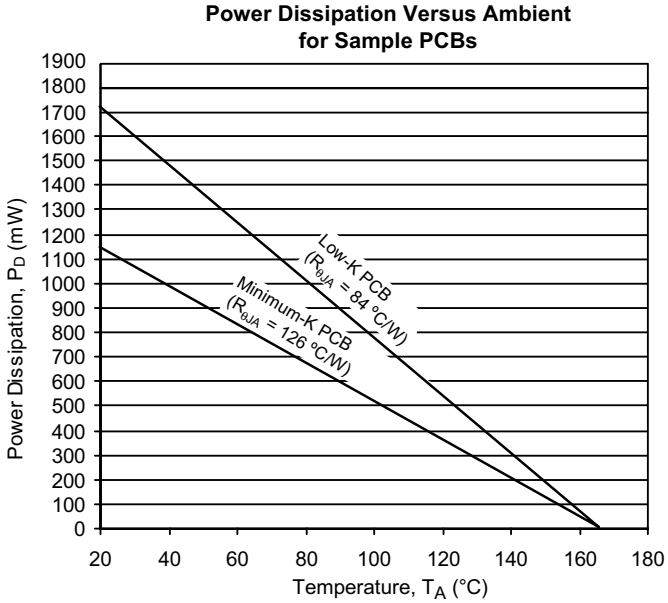

The device must be operated below the maximum junction temperature of the device, $T_{J(max)}$. Under certain combinations of peak conditions, reliable operation may require derating supplied power or improving the heat dissipation properties of the application. This section presents a procedure for correlating factors affecting operating T_J. (Thermal data is also available on the Allegro MicroSystems Web site.)

The Package Thermal Resistance, $R_{\theta JA}$, is a figure of merit summarizing the ability of the application and the device to dissipate heat from the junction (die), through all paths to the ambient air. Its primary component is the Effective Thermal Conductivity, K, of the printed circuit board, including adjacent devices and traces. Radiation from the die through the device case, $R_{\theta JC}$, is relatively small component of $R_{\theta JA}$. Ambient air temperature, T_A, and air motion are significant external factors, damped by overmolding.

The effect of varying power levels (Power Dissipation, P_D), can be estimated. The following formulas represent the fundamental relationships used to estimate T_J, at P_D.

$$P_D = V_{IN} \times I_{IN} \quad (1)$$

$$\Delta T = P_D \times R_{\theta JA} \quad (2)$$

$$T_J = T_A + \Delta T \quad (3)$$

For example, given common conditions such as: T_A= 25°C, V_{IN} = 12 V, I_{IN} = 4 mA, and $R_{\theta JA}$ = 140 °C/W, then:

$$P_D = V_{IN} \times I_{IN} = 12\ V \times 4\ mA = 48\ mW$$

$$\Delta T = P_D \times R_{\theta JA} = 48\ mW \times 140\ °C/W = 7°C$$

$$T_J = T_A + \Delta T = 25°C + 7°C = 32°C$$

A worst-case estimate, $P_{D(max)}$, represents the maximum allowable power level, without exceeding $T_{J(max)}$, at a selected $R_{\theta JA}$ and T_A.

Example: Reliability for V_{CC} at T_A=150°C, package SG, using minimum-K PCB.

Observe the worst-case ratings for the device, specifically: $R_{\theta JA}$=126°C/W, $T_{J(max)}$=165°C, $V_{CC(max)}$=26.5 V, and $I_{CC(max)}$ = 8 mA. Note that $I_{CC(max)}$ at T_A=150°C is lower than the $I_{CC(max)}$ at T_A=25°C given in the Operating Characteristics table.

Calculate the maximum allowable power level, $P_{D(max)}$. First, invert equation 3:

$$\Delta T_{max} = T_{J(max)} - T_A = 165\,°C - 150\,°C = 15\,°C$$

This provides the allowable increase to T_J resulting from internal power dissipation. Then, invert equation 2:

$$P_{D(max)} = \Delta T_{max} \div R_{\theta JA} = 15°C \div 126\ °C/W = 119\,mW$$

Finally, invert equation 1 with respect to voltage:

$$V_{CC(est)} = P_{D(max)} \div I_{CC(max)} = 119\,mW \div 8\,mA = 14.9\ V$$

The result indicates that, at T_A, the application and device can dissipate adequate amounts of heat at voltages ≤$V_{CC(est)}$.

Compare $V_{CC(est)}$ to $V_{CC(max)}$. If $V_{CC(est)} \leq V_{CC(max)}$, then reliable operation between $V_{CC(est)}$ and $V_{CC(max)}$ requires enhanced $R_{\theta JA}$. If $V_{CC(est)} \geq V_{CC(max)}$, then operation between $V_{CC(est)}$ and $V_{CC(max)}$ is reliable under these conditions.

Sensor Evaluation: EMC

Characterization Only

Test Name*	Reference Specification
ESD – Human Body Model	AEC-Q100-002
ESD – Machine Model	AEC-Q100-003
Conducted Transients	ISO 7637-1
Direct RF Injection	ISO 11452-7
Bulk Current Injection	ISO 11452-4
TEM Cell	ISO 11452-3

*Please contact Allegro MicroSystems for EMC performance

Package SG, 4-Pin SIP

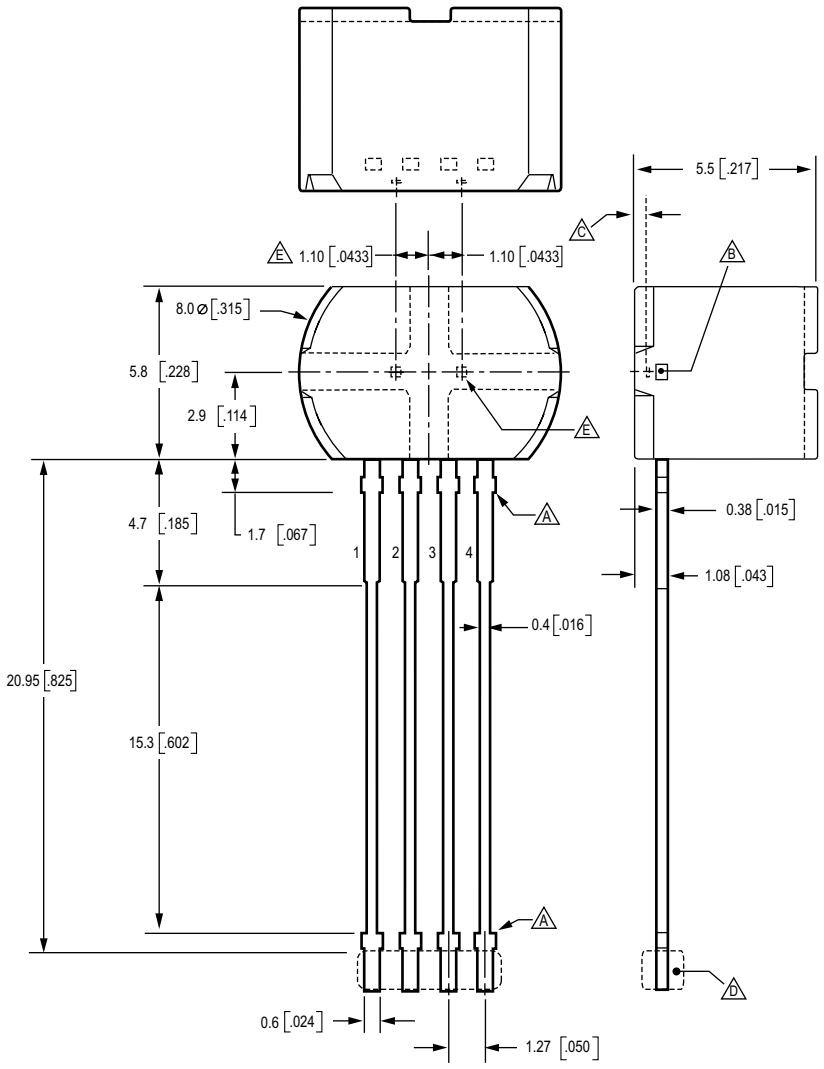

Preliminary dimensions, for reference only
Untoleranced dimensions are nominal.
Dimensions in millimeters
U.S. Customary dimensions (in.) in brackets, for reference only
Dimensions exclusive of mold flash, burrs, and dambar protrusions
Exact case and lead configuration at supplier discretion within limits shown

A Dambar removal protrusion (16X)
B Metallic protrusion, electrically connected to pin 4 and substrate (both sides)
C Active Area Depth, 0.43 [.017]
D Thermoplastic Molded Lead Bar for alignment during shipment
E Hall elements (2X)

The products described herein are manufactured under one or more of the following U.S. patents: 5,045,920; 5,264,783; 5,442,283; 5,389,889; 5,581,179; 5,517,112; 5,619,137; 5,621,319; 5,650,719; 5,686,894; 5,694,038; 5,729,130; 5,917,320; and other patents pending.

Allegro MicroSystems, Inc. reserves the right to make, from time to time, such departures from the detail specifications as may be required to permit improvements in the performance, reliability, or manufacturability of its products. Before placing an order, the user is cautioned to verify that the information being relied upon is current.

Allegro products are not authorized for use as critical components in life-support devices or systems without express written approval.

The information included herein is believed to be accurate and reliable. However, Allegro MicroSystems, Inc. assumes no responsibility for its use; nor for any infringement of patents or other rights of third parties which may result from its use.

Copyright © 2005, 2006 Allegro MicroSystems, Inc.